Semiconductor Physics, Quantum Electronics & Optoelectronics, 2024. V. 27, No 2. P. 208-215.

Hetero- and low-dimensional structures

Composite polymer films with semiconductor nanocrystals for organic electronics and optoelectronics

O.V. Pylypova[1], D.V. Korbutyak[2], V.S. Tokarev[3], A.I. Pylypov[4], A.A. Evtukh[1,2]

[1]*Educational and Research Institute of High Technologies, Taras Shevchenko National University of Kyiv, 01601 Kyiv, Ukraine*
[2]*V. Lashkaryov Institute of Semiconductor Physics, NAS of Ukraine, 03028 Kyiv, Ukraine*
[3]*Lviv Polytechnic National University, 79013 Lviv, Ukraine*
[4]*Dnipro University of Technology, 49005 Dnipro, Ukraine*
Corresponding author e-mail: olha.pylypova@knu.ua

Abstract. Organic materials and, in particular, polymer films enhanced with certain nanocrystals have a potential for wide application in electronics and optoelectronics due to their organic flexibility, lightweight, simple integration, affordable manufacturing cost, and low environmental impact of their production. The purpose of this research is to investigate the electrical properties of polymer-based composite films containing $Cd_{1-x}Cu_xS$ nanocrystals in order to determine their prospects for use as conductive layers in organic electronics and optoelectronics. The paper contains a detailed description of the synthesis method of hybrid nanocomposite films based on peroxide reactive copolymer (PRC) with $Cd_{1-x}Cu_xS$ nanocrystals. The defect structure of the films is studied by analyzing the photoluminescence spectra. Current-voltage characteristics of the films with different Cd and Cu contents in the $Cd_{1-x}Cu_xS$ nanocrystals embedded into the polymer matrix, deposited on glass substrates are measured in the dark and under light illumination. The film conductivity is found to increase with the Cu content in the $Cd_{1-x}Cu_xS$ nanocrystals. The carrier transport corresponds to the Ohm law at low voltages and the space charge limited current (SCLC) or Poole–Frenkel mechanisms at higher ones. The conductivity of the polymer-based hybrid nanocomposite films has a weak dependence on the intensity of light illumination. The explanation of the obtained experimental results is proposed.

Keywords: composite polymer films, nanocrystals, conductive layers, electrical conductivity, photoluminescence.

https://doi.org/10.15407/spqeo27.02.208
PACS 61.25.hp, 73.61.Ph, 78.55.Et, 82.35.Jk

Manuscript received 16.04.24; revised version received 18.05.24; accepted for publication 19.06.24; published online 21.06.24.

1. Introduction

Colloidal nanocrystals (NCs) have potential applications in optoelectronics, photovoltaics, biology, medicine, *etc*. [1]. Luminescent NCs based on II-VI compounds (CdSe, CdS, CdTe, and their alloys) are characterized by high quantum yield of photoluminescence (PL), narrow excitonic emission band, and wide absorption spectrum, which make them suitable for various applications [2].

An organic polymer matrix can stabilize nanoparticles embedded into it. The resulting nanocomposite can combine the properties of both organic and inorganic components, such as the mechanical properties of polymers and the optical and electrical properties of NCs. Incorporating semiconductor NCs into a solid structure offers certain advantages over nanoparticles in a solution. Solid matrices retain their shape. Moreover, polymer materials can be processed to obtain thin films, stretched and oriented, *etc*., which opens up new perspectives for fundamental research and some original applications [3]. The following compositions stand out: hybrid materials consisting of SiO_2/CdS particles dispersed in a (styrene-co-maleic anhydride) and a (styrene-co-maleimide) matrix [4], SiO_2 and titanium dioxide nanoparticles (TiO_2) embedded into a methyl ester (3-hexylthiophene) (P3HT) phenyl-C61-butyric acid (PC61BM) matrix [5], CdS-impregnated poly(vinylidene fluoride) PVDF (nano-CdS/PVDF) free-standing flexible films [3], and CdS NCs in a P3HT matrix [6, 7].

A number of studies show that embedding high-insulation and oriented CdS poly- or nanocrystals in efficient matrices (PVD) enables creating the most effective transducers in device technology [8]. The properties of polymer films have a number of advantages such as low cost, lightweight, large area and flexibility [9], and good environmental compatibility [10, 11].

The electrical properties of polymer-nanoparticle hybrids are often defined by the embedded nanoparticles or by nanoparticles interaction with the polymer matrix [12].

Long alkyl chains present in the trioctyl phosphine oxide ligands act as insulators and inhibit charge transfer between a nanocrystal and the conductive polymer (CP). Formation of direct bonds between the NCs and CP suppress the restrictive ligands effect [13]. In such films, charge transfer is more efficient and, hence, the efficiency increases [14, 15]. On the other hand, ligand exchange has some disadvantages, such as lack of morphology control and incomplete metabolic processes.

Current-voltage characteristics of polymer films with CdCuS nanoparticles were studied in a number of publications [16–22]. A nanosized composite sensitizer composed of CuS and CdS quantum dots was obtained by layer-by-layer deposition utilizing the interaction between metal cations (Cu^{2+} or Cd^{2+}) and sulfide anions (S^{2+}). Such sensitizer showed an increased by an order of magnitude current density under light illumination as compared to that of pure CdS sensitizer [16]. The polyvinyl alcohol polymer/CuS thin films synthesized at the CuS concentration of 0.2 g exhibited the largest grain size (37.3 nm), the highest thickness (17.48 μm), low conductivity, mobility and carrier concentration (2.8 Ohm·cm, $7.55 \cdot 10^3$ $cm^2/V \cdot s$, and $1.48 \cdot 10^{14}/cm^3$), the lowest bandgap (3.59 eV), and the strongest emission bands [17]. It was discovered that the conduction mechanism of the PVA/PANI@CuS hybrid nano-composites corresponded to the Poole–Frenkel one [19].

The goal of this work is to investigate the electrical properties of polymer-based composite films containing $Cd_{1-x}Cu_xS$ nanocrystals to determine their prospects for organic electronics and optoelectronics. The important feature of the films under investigation is the formation of NCs inside the polymer matrix *via in-situ* reactions.

2. Experimental

Nanocomposite polymer films with embedded semiconductor $Cd_{1-x}Cu_xS$ NCs were prepared in several stages. At the beginning, a solution of peroxide reactive copolymer (PRC, see Fig. 1), polyethylene glycol (PEG-200, Fig. 1) and a mixture of cadmium acetate ($CdAc_2$) with copper acetate ($CuAc_2$) in dimethylformamide were prepared at different $Cd(Ac)_2$:$Cu(Ac)_2$ ratios. Due to dissociation of $Cd(Ac)_2$ and $Cu(Ac)_2$ in the solution, Cd^{2+} and Cu^{2+} ions bound to a polymer matrix formed. After that, thin polymer films containing Cd^{2+} and/or Cu^{2+} cations were deposited by spin coating on glass plates.

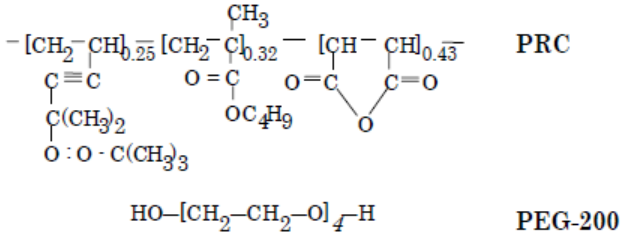

Fig. 1. Chemical structures of the used polymers.

At the second stage, these films were annealed and crosslinked at T = 393 K for 2 hours. It was found that the high degree of crosslinking of the polymer films was achieved due to the: (i) interaction of the PEG-200 hydroxyl groups with the PRC anhydrous functional substances and (ii) sequence of radical reactions involving disintegration of the PRC peroxide functionals. The content of the gel fraction in the crosslinked polymer films reached 96% and higher. Afterwards, semiconductor NCs were formed inside the polymer films by exposure to hydrogen sulfide (H_2S) for 6 hours at 60 °C. The theoretical NCs content in the polymer films was estimated to be 20%. At the last stage, nanocomposite polymer films with embedded semiconductor $Cd_{1-x}Cu_xS$ NCs were prepared.

PL spectra were measured on an automated installation consisting of a modulated light source (helium-cadmium laser LH-70, 325.0 nm, 10 mW output), monochromator, photodetector, amplifier, and PC controller.

Current-voltage characteristics of the films with different ratios of Cd and Cu in the $Cd_{1-x}Cu_xS$ NCs embedded into the polymer matrix, deposited on glass substrates were measured without and under light illumination using a picoampermeter Keithley 2410 in two-contact probe configuration. A solar light simulator with the light intensity of 100 mW/cm^2 based on halogen lamps was used for illuminating the samples.

3. Results and discussion

3.1. Photoluminescence spectra

PL spectra of the $Cd_{1-x}Cu_xS$ NCs (x = 0, 0.5, 1) measured at T = 300 K are presented in Fig. 2. As can be seen from this figure, the spectra are quite similar and consist of two parts, namely an exciton band E (420…500 nm) and impurities-bound exciton bands D_1 and D_2 (500…650 nm). The PL intensity of the nanocomposite thin films significantly increases with the concentration of the $Cd_{1-x}Cu_xS$ NCs. Similar PL bands were observed in [23] for CdS NCs doped with Cu. The PL impurity bands D_1 and D_2 are caused by radiative recombination of non-equilibrium charge carriers on the CdS NCs surface defects [24]. However, the nature of the radiative recombination centers in CdS NCs and ternary compounds based on them is not yet understood.

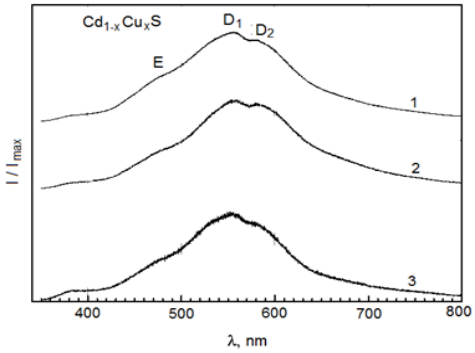

Fig. 2. Photoluminescence spectra of $Cd_{1-x}Cu_xS$ NCs embedded in polymer film: *1* – CdS, $x = 0$; *2* – $Cd_{1-x}Cu_xS$, $x = 0.5$; *3* – CuS, $x = 1$ ($T = 300$ K).

Some assumptions on the nature of PL have been made. Luminescence through surface defects of undetermined nature [25], through complex V_{Cd}-V_S centers [26], and through V_{Cd} acceptor centers [27–29] has been considered. The results obtained in this work indicate that the impurity PL (D_1 and D_2 bands) of the $Cd_{1-x}Cu_xS$ NCs is not associated with V_{Cd}. As can be seen from Fig. 2, the impurity bands D_1 and D_2 are observed in both cases of the CdS ($x = 0$) and CuS ($x = 1$) NCs. We believe that these bands are caused by recombination centers created by excess interstitial sulfur atoms. A similar interpretation has been proposed for single crystalline CdS semiconductors [29, 30]. In our case, creation of internal defects by interstitial sulfur atoms is likely enough, because formation of the $Cd_{1-x}Cu_xS$ NCs takes place during annealing in H_2S at the third stage. In the framework of the proposed model of radiative recombination in the $Cd_{1-x}Cu_xS$ NCs, the impurity-bound exciton bands of the PL spectra are attributed to capture of non-equilibrium charge carriers (electrons) by local centers created by interstitial sulfur ions incoming from the gas phase.

3.2. Electrical conductivity

Light and dark log *J*–*E* characteristics of the polymer films with embedded $Cd_{1-x}Cu_xS$ NCs with different Cu concentrations are presented in Fig. 3. The dependence of the current density on the applied field is similar to that for poly(3-hexylthiophene (P3HT) polymer films with CdS NCs [31].

As can be seen from Fig. 3, the values of current increase with the Cu content in the $Cd_{1-x}Cu_xS$ NCs. We analyze the current transport mechanism for three types of $Cd_{1-x}Cu_xS$ NCs: I – $x = 0$ and $x = 0.25$, II – $x = 0.40$ and $x = 0.6$, III – $x = 1$ (Figs. 3a and 3b). The conductivity difference between two neighboring sample types in the sequence is 2 orders of magnitude.

Type I (0…25% Cu in the $Cd_{1-x}Cu_xS$ NCs). The current-voltage characteristics under illumination of such composite films in the log*J*–log*U* scale are presented in Fig. 4. As can be seen from this figure, the current changes with applied voltage according to the Ohm law at small applied voltages.

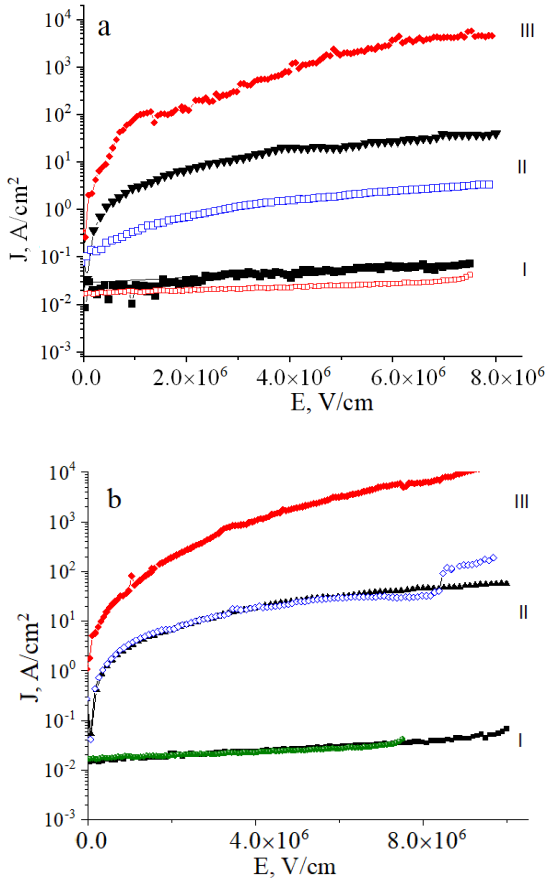

Fig. 3. *J*–*E* characteristics of $Cd_{1-x}Cu_xS$ NCs: I – $x = 0$ and $x = 0.25$, II – $x = 0.50$ and $x = 0.7$, III – $x = 1$. a) in the dark, b) under light illumination.

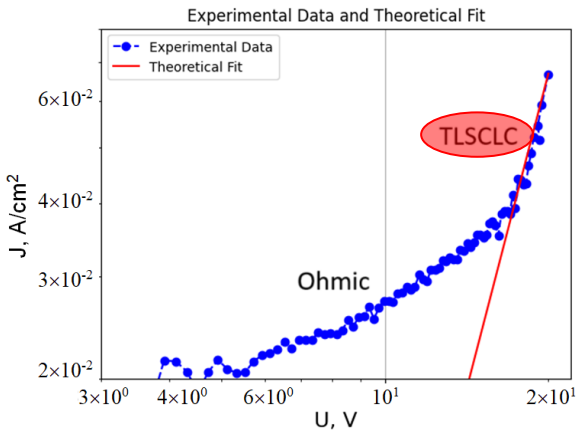

Fig. 4. Experimental (symbols) and calculated (straight line) *J*–*U* characteristics of composite polymer films with $Cd_{1-x}Cu_xS$ NCs measured under light illumination at 290 K.

With subsequent growth of applied voltage, the injected carrier density increases, and at the voltage corresponding to the change of the slope the concentration of injected carriers is equal to the thermally generated carriers [32]. At this applied voltage, the conductivity goes from the Ohm law to the space charge

limited current (SCLC) transport mechanism (Fig. 4). The expression for current density at the TL SCLC mechanism is given by [32–35]:

$$j = q^{1-l}\mu N_v\left(\frac{2l+1}{l+1}\right)^{l+1}\left(\frac{l}{l+1}\frac{\varepsilon_r\varepsilon_0}{N_t}\right)^{l}\frac{V^{l+1}}{d^{2l+1}}, \quad (1)$$

where N_t is the trap density, ε_0 is the permittivity of free space, ε_r is the film dielectric constant, μ is the carrier mobility, N_v is the density of states in the respective band, d is the sample thickness, and $l = T_c/T$, where T is the measurement temperature and T_c is the characteristic temperature, respectively. T_c is related to the characteristic energy of the trap distribution as $E_t = k_B T_c$ and $l = E_t/k_B T = T_c/T$, where k_B is the Boltzmann constant. Eq. (1) predicts a J–U^m dependence, where $m = l + 1$. Hence, the slope of a J–U dependence in the log-log coordinates directly determines the characteristic temperature and energy.

In case of exponential distribution of traps on energy, the distribution function is described as follows [31, 32]:

$$N_t(E) = (N_b/E_t)\exp(-E/E_t), \quad (2)$$

where $N_t(E)$ is the distribution function of the hole trap density at the energy level E above the valence band edge (assuming uniform spatial distribution), N_b is the density of traps at the edge of the valence band, and E_t is the characteristic trap energy, respectively.

The onset voltage (V_0) for the transition from the Ohm law to the TL SCLC mechanism is given by [32]

$$V_0 = \frac{q N_b d^2}{\varepsilon}\left(\frac{p_0}{N_v}\right)^{1/l}\left(\frac{l+1}{l}\right)\left(\frac{l+1}{2l+1}\right)^{l+1/l}. \quad (3)$$

The solid line in Fig. 4 is calculated based on Eq. (1). The values of the parameters used in the calculations are: $N_b = 7.9\cdot10^{10}$ cm^{-3}, $N_v = 8\cdot10^{8}$ cm^{-3}, $\varepsilon = 3.2$, $\varepsilon_0 = 8.85\cdot10^{14}$ F/cm, $\mu = 1.5\cdot10^{-5}$ cm^2 V$^{-1}\cdot$s, $d =$ 20 nm, and $T_c = 754$ K, which corresponds to $E_t = 0.064$ eV. As can be seen from Fig. 4, the experimental data have a good agreement with the TL SCLC carrier transport mechanism.

The hole transport parameters, namely the trap density (N_b) and the trap characteristic energy (E_t), can be understood analyzing charge transfer between the host (PRC) and the guest (CdS). Formation of charge transfer complexes between the host and the guest may be the dominant mechanism of interaction between them [31].

Guest CdS NCs can create favorable energy states within the forbidden band (traps) of the primary PCR. These states lead to the increase in the trap density (N_b) and trap characteristic energy (E_t) as shown in Fig. 5. Due to the very high trap density, the quantity of injected charge carriers is insufficient to fill all the trap states. This is why charge transport in the PRC-CdS composite polymer film is governed by the TL SCLC mechanism.

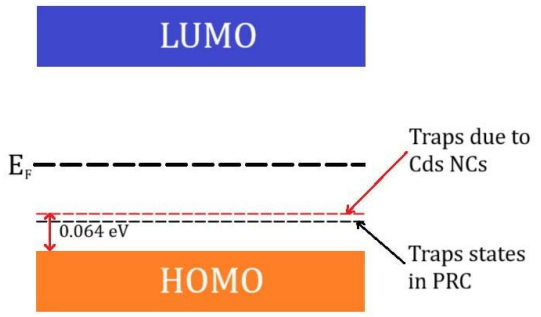

Fig. 5. Schematics of trap distribution and characteristic energy in the bandgap of PRC-CdS polymer composite.

Type II (40%, 60% Cu in the $Cd_{1-x}Cu_xS$ NCs). In the case of the PRC-$Cd_{1-x}Cu_xS$ composite polymer films with 40–60% of Cu in the $Cd_{1-x}Cu_xS$ NCs, the carrier transport according to the Ohm law dominates within the investigated voltage range for the measurements both without and under light illumination (Fig. 6).

The current-voltage dependence can be described by the following equation [32]:

$$J = en_0\mu\frac{U}{d}, \quad (4)$$

where J is the current density, U is the voltage, e is the elementary charge, n_0 is the free carrier (electron or holes) concentration, μ is the carrier mobility, and d is the film thickness, respectively.

The free carrier concentrations can be estimated by postulating the carrier mobility in polymers at the level of $\mu = 1.5\cdot10^{-5}$ cm^{2}V^{-1}s^{-1} as calculated from the TL SCLC model. This value is in agreement with the one obtained in [31, 33]. The values of n_0 calculated from the slopes of the curves in Fig. 6 are provided in Table.

Type III (CuS NCs). In this case, the current-voltage characteristics are linearized in the log (I/U)–$U^{1/2}$ coordinates (Fig. 7). This evidences the conduction according to the Poole–Frenkel mechanism [35–37]:

$$I \sim U\exp\left[-\frac{q\varphi_B}{kT} + \frac{q\sqrt{qU/d\pi\varepsilon_r\varepsilon_0}}{kT}\right], \quad (5)$$

where φ_B is the barrier height.

Table. Free carrier concentration n_0 in PRC-$Cd_{1-x}Cu_xS$ composite polymer films with 40% and 60% of Cu in $Cd_{1-x}Cu_xS$ NCs.

Cu in $Cd_{1-x}Cu_xS$ nanocrystals	In the dark, n_0, cm^{-3}	Under light illumination, n_0, cm^{-3}
40%	$3.4\cdot10^{10}$	$4.0\cdot10^{11}$
60%	$1.2\cdot10^{13}$	$6.9\cdot10^{13}$

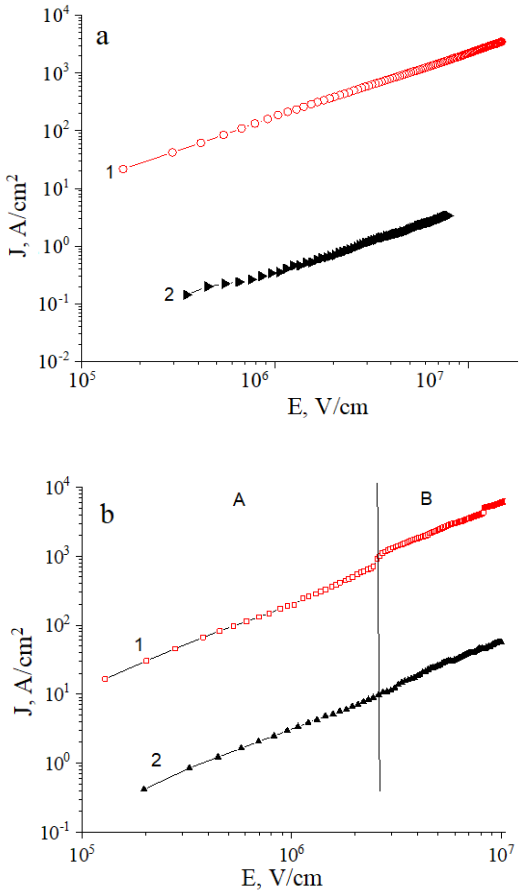

Fig. 6. Current-voltage characteristics of PRC-$Cd_{1-x}Cu_xS$ composite polymer film in log–log coordinates: *1* – x = 0.6, *2* – x = 0.4 in the dark (a) and under light illumination (b).

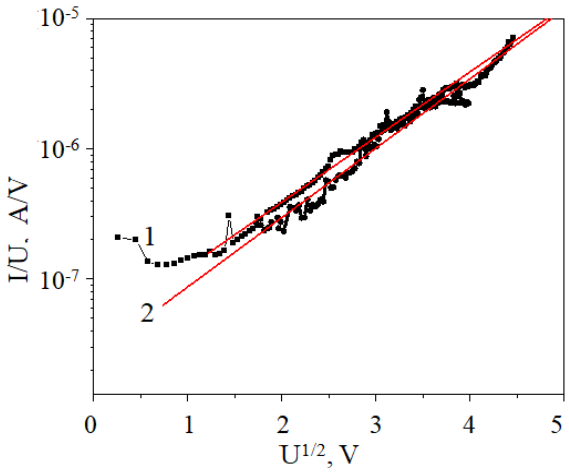

Fig. 7. Current-voltage characteristics in Poole–Frenkel coordinates for PRC-CuS composite polymer film with CuS NCs: *1* – under light illumination, *2* – in the dark.

The barrier height was determined from the intercept of the curves with the ordinate axis in the Poole–Frenkel coordinates (Fig. 7). The obtained barrier heights for the composite polymer film with CuS NCs are $\varphi_B \approx 0.42$ eV (under light illumination) and $\varphi_B \approx 0.44$ eV (in the dark). These barriers form between the trapping centers and the lowest unoccupied molecular orbitals (LUMO) band in the PRC-CuS composite polymer film.

Different nature of the traps taking part in the conduction is caused by the peculiarities of the interaction of the CdS and CuS NCs with the polymer matrix. An increase of the Cu content in the $Cd_{1-x}Cu_xS$ NCs causes a decrease of the concentration of interstitial sulfur atoms in the polymer matrix due to the higher reactivity of Cu with sulfur as compared to Cd. In such a way, the density of local energy centers in bandgap and NC – polymer interfaces are decreased. The dissociation energy of a Cu-S bond is 285 kJ/mol as compared to 195 kJ/mol for a Cd-S bond. The slight dependence of the PL spectra on the Cu content in the $Cd_{1-x}Cu_xS$ NCs and strong dependence of the conductivity allows one to conclude that different trap centers are involved in the PL and conductivity processes.

4. Conclusions

Organic materials such as polymers enhanced with nanocrystals demonstrate a variety of properties that make them a viable option for application in optoelectronics. Following this path of research, we have synthesized hybrid nanocomposite films based on the polymer films containing $Cd_{1-x}Cu_xS$ NCs. The contents of Cd and Cu in the $Cd_{1-x}Cu_xS$ NCs were varied by varying the ratio of cadmium acetate and copper acetate during preparation.

PL spectra of these hybrid nanocomposite films in the wavelength range of 420…650 nm have been measured. In the framework of the proposed model of radiative recombination in the $Cd_{1-x}Cu_xS$ NCs, the impurity-bound exciton bands of the PL spectra are attributed to capture of non-equilibrium charge carriers (electrons) by local centers created by interstitial sulfur ions. This interpretation correlates with the interpretation of impurity-bound exciton bands of PL spectra of single crystalline CdS semiconductors.

Increase in the electrical conductivity of the studied films with the growth of Cu content in the $Cd_{1-x}Cu_xS$ NCs has been found and explained by the increase of free carrier concentration. Electron transport through the films obeys the Ohm law at lower voltages. The space charge limited current transport mechanism dominates at higher voltages. The Poole–Frenkel electron transport mechanism was identified in the case of the PRC-CuS composite polymer films.

It follows from the above-mentioned results that the studied hybrid nanocomposite films may be used in organic polymer-based electronics and optoelectronics as conductive layers with electrical conductivity varying in a wide (some orders of magnitude) range.

Funding and Conflicts of interests

This work was partly supported by the project No. M/74-2023 of the Ministry of Education and Science of Ukraine. The authors declare no conflict of interests.

Data availability

The datasets used and/or analyzed in this study are available from the corresponding author on reasonable request.

References

1. Xu J., Wang S., Wang, G.J.N. *et al.* Highly stretchable polymer semiconductor films through the nanoconfinement effect. *Science*. 2017. **355**. P. 59–64. https://doi.org/10.1126/science.aah4496.
2. Mattoussi H., Palui G., Na H.B. Luminescent quantum dots as platforms for probing *in vitro* and *in vivo* biological process. *Adv. Drug Deliv. Rev.* 2012. **64**. P. 38–166. https://doi.org/10.1016/j.addr.2011.09.011.
3. Akperov O.H., Muradov M.B., Malikov E.Y. *et al.* Synthesis and characterization of CdS nanocrystals in Maleic anhydride–Octene-1–Vinylbutyl Ether terpolymer matrix. *Phys. E: Low-Dimens.* 2016. **81**. P. 150–155. https://doi.org/10.1016/j.physe.2016.03.012.
4. Pileni M.P. (Ed.). *Nanocrystals Forming Mesoscopic Structures*. John Wiley & Sons, 2006.
5. Garg M., Padmanabhan V. Poly (3-hexylthiophene) (P3HT) and phenyl-C61-butyric acid methyl ester (PC61BM) based bulk heterojunction solar cells containing silica and titanium dioxide nanorods: Molecular dynamics simulations. *J. Nanosci. Nanotechnol*. 2020. **20**. P. 858–870. http://doi.org/10.1166/jnn.2020.16892.
6. Khan M.T., Kaur A., Dhawan, S.K., Chand S. In-situ growth of cadmium telluride nanocrystals in poly (3-hexylthiophene) matrix for photovoltaic application. *J. Appl. Phys.* 2011. **110**. P. 044509. https://doi.org/10.1063/1.3626464.
7. Jung J. Preparation of anisotropic CdSe-P3HT core-shell nanorods using directly synthesized Br-functionalized CdSe nanorods. *Surf. Coat. Technol.* 2019. **362**. P. 84–89. https://doi.org/10.1016/j.surfcoat.2019.01.093.
8. Bhunia R., Ghosh D., Ghosh B. *et al.* Some aspects of microstructural and dielectric properties of nanocrystalline CdS/poly (vinylidene fluoride) composite thin films. *Polym. Int*. 2015. **64**. P. 924–934. https://doi.org/10.1002/pi.4866.
9. Liu T., Xue X., Huo L. *et al.* Highly efficient parallel-like ternary organic solar cells. *Chem. Mater.* 2017. **29**. P. 2914–2920. https://doi.org/10.1021/acs.chemmater.6b05194.
10. Sun B., Zou G., Shen X., Zhang X. Exciton dissociation and photovoltaic effect in germanium nanocrystals and poly (3-hexylthiophene) composites. *Appl. Phys. Lett.* 2009. **94**. P. 233504. https://doi.org/10.1063/1.3152997.
11. Shiri P., Dacanay E.J.S., Hagen B., Kaake L.G. Dynamic charging mechanism of organic electro-chemical devices revealed with in situ infrared spectroscopy. *J. Phys. Chem.* 2019. **123**. P. 19395–19401. https://doi.org/10.1021/acs.jpcc.9b05739.
12. Liu K., Chu L.H., Jiang B. *et al.* $Li_{1.4}Al_{0.4}Ti_{1.6}(PO_4)_3$ nanoparticles reinforced solid polymer electrolytes for all-solid-state lithium batteries. *Solid State Ionics*. 2019. **331**. P. 89–95. https://doi.org/10.1016/j.ssi.2019.01.007.
13. Lee Y.P., Liu M.W., Qin J.K. *et al*. Long-term thermally stable nanoconfining networks for efficient fully conjugated semicrystalline/amorphous diblock copolymer photovoltaics. *Org. Electron.* 2019. **69**. P. 263–274. https://doi.org/10.1016/j.orgel.2019.02.016.
14. Nguyen M.T., Jones R.A., Holliday B.J. Direct synthesis of CdSe nanocrystals within a conducting metallopolymer: toward improving charge transfer in hybrid nanomaterials. *Chem. Comm.* 2016. **52**. P. 13112–13115. https://doi.org/10.1039/C6CC07193G.
15. Lu K. Hybrid materials – a review on co-dispersion, processing, patterning, and properties. *Int. Mater. Rev.* 2019. **65**. P. 1–39. https://doi.org/10.1080/09506608.2019.1653569.
16. Malathi A., Madhavan J. Synthesis and characterization of CuS/CdS photocatalyst with enhanced visible light-photocatalytic activity. *J. Nano Res.* 2017. **48**. P. 49–61. https:// doi.org/10.4028/www.scientific.net/JNanoR.48.49.
17. Sabah F.A., Razak I.A., Kabaa E.A., Zaini M.F., Omar A.F. Influence of CuS powder concentration on the construction of hybrid PVA/CuS thin films for polymer light-emitting applications. *J. Mater. Sci.: Mater. Electron*. 2020. **31**. P. 3456–3465. https://doi.org/10.1007/s10854-020-02893-y.
18. Gu J., Ying M., Zhao Y. The influence of post-treatment processes on the structures and the optical and electrical properties of $CuInS_2$ and its heterojunction with various sulfides (CdS, CdZnS, and CdCuS). *J. Sol-Gel Sci. Technol.* 2021. **97**. P. 672–684. https://doi.org/10.1007/s10971-021-05473-6.
19. Sangamesha M.A., Rajanna K., Shivaraju V.K., Madhukar B.S. Preparation and characterization of down converting poly (vinyl alcohol)/PANI@CuS hybrid nanocomposites for optoelectronic application. *Chem. Inorgan. Mater*. 2023. **1**. P. 100025. https://doi.org/10.1016/j.cinorg.2023.100025.
20. Wang G., Morrin A., Li M., Liu N., Luo X. Nanomaterial-doped conducting polymers for electrochemical sensors and biosensors. *J. Mater.*

Chem. B. 2018. **6**, No 25. P. 4173–4190. https://doi.org/10.1039/C8TB00817E.
21. Liang Y.Y., Xu Z., Xia J.B. *et al*. For the bright fullerene bulk heterojunction polymer solar cells with power conversation efficiency of 7.4%. *Adv. Mat.* 2010. **22**. P. E135–E138. https://doi.org/10.1002/adma.200903528.
22. Gusain A., Faria R.M., Miranda P.B. Polymer solar cells – interfacial processes related to performance issues. *Front. Chem.* 2019. **7**. https://doi.org/10.3389/fchem.2019.00061.
23. Agrawal S., Srivastava S., Kumar S. *et al*. Swift heavy ion irradiation effect on Cu-doped CdS nanocrystals embedded in PMMA. *Bull. Mater. Sci.* 2009. **32.** P. 569–573. https://doi.org/10.1007/s12034-009-0086-9.
24. Korbutyak D.V., Kladko V.P., Safryuk N.V. *et al*. Synthesis, luminescent and structural properties of the $Cd_{1-x}Cu_xS$ and $Cd_{1-x}Zn_xS$ nanocrystals. *J. Nano- Electron. Phys*. 2017. **9**. P. 05024. https://doi.org/10.21272/jnep.9(5).05024.
25. Muruganandam S., Anbalagan G., Murugadoss G. Synthesis and structural, optical and thermal properties of CdS:Zn^{2+} nanoparticles. *Appl. Nanosci*. 2014. **4**. P. 1013–1019. https://doi.org/10.1007/s13204-013-0284-z.
26. Smyntyna V., Skobeeva V., Malushin N. The nature of emission centers in CdS nanocrystals. 2007. **42**. P. 693–696. https://doi.org/10.1016/j.radmeas.2007.01.068.
27. Mandal P., Talwar S.S., Major S.S., Srinivasa R.S. Orange-red luminescence from Cu doped CdS nanophosphor prepared using mixed Langmuir–Blodgett multilayers. *J. Chem. Phys*. 2008. **128**. P. 114703. https://doi.org/10.1063/1.2888930.
28. Lee H., Yang H., Holloway P.H. Functionalized CdS nanospheres and nanorods *Physica B: Condensed Matter*. 2009. **404**. P. 4364–4369. https://doi.org/10.1016/j.physb.2009.09.020.
29. Yuan S.Q., Ji P.F., Li Y. *et al*. Unusual blueshifting of optical band gap of CdS nanocrystals through a chemical bath deposition method. *Adv. OptoElectron.* 2015. **2015**. Art. ID 317108. https://doi.org/10.1155/2015/317108.
30. Kulp B.A., Kelley H. Displacement of the sulfur atom in CdS by electron bombardment. *J. Appl. Phys.* 1960. **31**. P. 1057–1061. https://doi.org/10.1103/PhysRev.125.1865.
31. Khan M.T., Almohammedi A. Effect of CdS on charge transport in poly(3-hexylthiophene). *J. Appl. Phys.* 2017. **132**. P. 075502. https://doi.org/10.1063/1.4999316.
32. Lampert M.A., Mark. P. *Current Injection in Solids*. Academic, New York, 1970. P. 1–96. https://doi.org/10.1016/S0080-8784(08)62630-7.
33. Zheng Y.Q., Lei T., Dou J.H. *et al*. Strong electron-deficient polymers lead to high electron mobility in air and their morphology-dependent transport behaviors. *Adv. Mater*. 2016. **28**. P. 7213–7219.
34. Abd El-Kader F.H., Hamza S.S., Attia G. Electrical and optical studies on γ-irradiated pure and chromium-chloride-doped polyvinyl alcohol. *J. Mater. Sci.* 1993. **28**. P. 6719–6723. https://doi.org/10.1007/BF00356421.
35. Kizjak A., Evtukh A., Steblova O., Pedchenko Yu. Electron transport through thin SiO_2 films containing Si nanoclusters. *J. Nano Res.* 2016. **39**. P. 169–177. https://doi.org/10.4028/www.scientific.net/JNanoR.39.169.
36. Gaspar H., Figueira F., Pereira L. *et al*. Recent developments in the optimization of the bulk heterojunction morphology of polymer: Fullerene solar cells. *Materials.* 2018. **11**. P. 2560. https://doi.org/10.3390/ma11122560.
37. Gavrylyuk O.O., Semchyk O.Y., Bratus O.L. *et al*. Study of thermophysical properties of crystalline silicon and silicon-rich silicon oxide layers. *Appl. Surf. Sci*. 2014. **302**. P. 213–215. https://doi.org/10.1016/j.apsusc.2013.09.171.

Authors and CV

Olha Pylypova, defended her Ph.D. thesis in Physics and Mathematics (Semiconductor Physics) at the Educational and Research Institute of High Technologies, Taras Shevchenko National University of Kyiv in 2016. She is an Assistant Professor at the same university. Authored over 69 publications and 2 textbooks. The area of her scientific interests includes physics and technology of semiconductor materials, such as SiO_x and hybrid structures and devices (solar cells, photoresistors, light-emitted structures *etc*.), as well as analysis, diagnostics, modeling and forecasting physical processes in different objects.
https://orcid.org/0000-0002-0337-4724

Dmytro Korbutyak, Professor, Doctor of Physical and Mathematical Sciences, Laureate of the State Prize of Ukraine in Science and Technology, Chief Researcher at the Department of Surface Physics and Nanophotonics of the V. Lashkaryov Institute of Semiconductor Physics, NAS of Ukraine. His main scientific works are devoted to the study of the luminescence properties of non-doped and doped with various impurities A^2B^6 nanocrystals, hybrid semiconductor-metal nanostructures, as well as to the elucidation of the mechanisms of radiative processes in semiconductor nanocrystals. He is the author of two monographs and over 300 scientific works in the field of semiconductor physics and nanocrystals.
E-mail: dmytro.korbutyak@gmail.com

Victor Tokarev, defended his Doctor of Sciences thesis in Chemistry in 2006 at the Lviv Polytechnic National University. He is a Professor at the Organic Chemistry Department of the Institute of Chemistry and Chemical Technologies at the same university. His main research activity is in the field of synthesis of reactive polymers, modification of surfaces with polymers, thin polymer films, dispersion polymerization, polymerization at phase interfaces, filled composite materials, conductive polymers, colloids, semiconductor nanoclusters and quantum dots, and nanocomposites.
E-mail: viktor.s.tokariev@lpnu.ua

Anton Pylypov, defended his Master thesis in 2010 at the Department of Electricity Systems, Dnipro University of Technology. The area of his scientific interests includes physics and technology of semiconductor materials, electronics devices and sensors (photoresistors, light-emitted structures *etc*.), as well as analysis, diagnostics, modeling and forecasting physical processes in different objects, circuitry, electronics and modern element base.
E-mail: pylypov.anton@gmail.com,
https://orcid.org/0009-0009-2996-1503

Anatoliy Evtukh, defended his PhD thesis in Physics and Mathematics (Physics of Semiconductors and Dielectrics) at the V. Lashkaryov Institute of Semiconductor Physics, NAS of Ukraine in 1985 and Doctor of Sciences thesis at the same institute in 2004. He is a Leading Researcher at the Department of Physics of Surface and Nanophotonics of the same institute. Authored over 300 publications. His main research activity is in the field of nanomaterials and nanostructures, composite films with semiconductor and metal nano-inclusions, electron transport, surface physics, semiconductor technologies, sensors and solar cells. E-mail: anatoliy.evtukh@gmail.com, https://orcid.org/0000-0003-3527-9585

Authors' contributions

Pylypova O.V.: measurement of current-current characteristics and analysis of electrical conductivity, writing – review & editing.
Korbutyak D.V.: key idea, conceptualization, photoluminescence analysis.
Tokarev V.S.: key idea, synthesis of composite polymer films.
Pylypov A.I.: theoretical modeling and analysis of electrical conductivity.
Evtukh A.A.: conceptualization, analysis, validation, writing – review & editing.

Композитні полімерні плівки з напівпровідниковими нанокристалами для органічної електроніки та оптоелектроніки

О.В. Пилипова, Д.В. Корбутяк, В.С. Токарєв, А.І. Пилипов, А.А. Євтух

Анотація. Органічні матеріали, зокрема полімерні плівки, вдосконалені нанокристалами, мають потенціал для широкого застосування в електроніці та оптоелектроніці завдяки своїй органічній гнучкості, легкій вазі, простішій інтеграції, більш доступній вартості виробництва та низькому впливу на навколишнє середовище їх виробництва. Метою даного дослідження є дослідження електричних властивостей композитних плівок на полімерній основі, що містять нанокристали $Cd_{1-x}Cu_xS$, з метою визначення перспектив їх використання в органічній електроніці та оптоелектроніці як провідний шар. Стаття містить докладний опис синтезу гібридних нанокомпозитних плівок на основі пероксид-реактивного кополімеру (PRC) з нанокристалами $Cd_{1-x}Cu_xS$. Дефектну структуру плівок аналізували за спектрами фотолюмінесценції. Виміряно світлову і темнову вольт-амперні характеристики цих плівок із різним співвідношенням Cd і Cu в нанокристалах $Cd_{1-x}Cu_xS$, вбудованих у полімерну матрицю та нанесених на скляні підкладки. Встановлено, що провідність плівок зростає зі зростанням вмісту Cu в нанокристалах $Cd_{1-x}Cu_xS$. Електронний транспорт відповідає закону Ома при низьких напругах та механізмам струму, обмеженого просторовим зарядом, чи Пула–Френкеля при високих напругах. Провідність цих гібридних нанокомпозитних плівок на полімерній основі слабо залежить від світла. Запропоновано пояснення отриманих експериментальних результатів.

Ключові слова: композитні полімерні плівки, нанокристали, провідні шари, електропровідність, фотолюмінесценція.